PROCEEDINGS OF SPIE

SPIEDigitalLibrary.org/conference-proceedings-of-spie

Enhanced Raman techniques for infection diagnostics

Niall Hanrahan, Adam Lister, Callum Highmore, Leena Rajith, Ekaterina Avershina, et al.

Niall Hanrahan, Adam Lister, Callum Highmore, Leena Rajith, Ekaterina Avershina, Jawad Ali, Rafi Ahmad, Jeremy Webb, Sumeet Mahajan, "Enhanced Raman techniques for infection diagnostics," Proc. SPIE 12203, Enhanced Spectroscopies and Nanoimaging 2022, 1220303 (3 October 2022); doi: 10.1117/12.2635324

SPIE.

Event: SPIE Nanoscience + Engineering, 2022, San Diego, California, United States

Enhanced Raman techniques for infection diagnostics

Niall Hanrahan*[a,b], Adam Lister[a,b], Callum Highmore[c,d], Leena Rajith[e], Ekaterina Avershina[f], Jawad Ali[f], Rafi Ahmad[f,g] Jeremy Webb[c,d], Sumeet Mahajan**[a,b]

[a] Institute for Life Sciences (IfLS), University of Southampton, University Road, Southampton, Hants., UK, SO17 1BJ;

[b] School of Chemistry, University of Southampton, University Road, Southampton, Hants., UK, SO17 1BJ;

[c] National Biofilms Innovation Centre (NBIC), University of Southampton, University Road, Southampton, Hants., UK, SO17 1BJ;

[d] School of Biological Sciences, University of Southampton, University Road, Southampton, Hants., UK, SO17 1BJ;

[e] Department of Applied Chemistry, Cochin University of Science and Technology, Kalamassery, Kochi-22, Kerala, India;

[f] Department of Biotechnology, Inland Norway University of Applied Sciences, Holsetgata 22, 2317, Hamar, Norway;

[g] Institute of Clinical Medicine, Faculty of Health Sciences, UiT - The Arctic University of Norway, Hansine Hansens veg 18, 9019, Tromsø, Norway;

*n.hanrahan@soton.ac.uk; **s.mahajan@soton.ac.uk;

ABSTRACT

In this paper we describe our recent work in multi-excitation surface enhanced Raman spectroscopy (MX-SERS), and its application for robust strain-level bacteria identification. The development of MX-SERS follows directly from our previous work in rapid bacterial identification using multi-excitation Raman spectroscopy (MX-Raman), which enabled highly accurate (up to 99.75%) strain-level distinction of bacteria, including antibiotic resistant strains of bacteria and from within complex media. In this work we use the strong wavelength dependence of both the Raman scattering cross-section and the surface plasmon to demonstrate a novel capability in bacteria identification. Compared to MX-Raman, MX-SERS has up to 8x faster data acquisition speed as well as up to 4000x lower laser power incident on the sample. Furthermore, we fabricate SERS-active substrates with a simple and low-cost fabrication method that can be adapted to fit a chosen wavelength regime. This combination of strain-level sensitivity and high-speed detection, combined with a low-cost SERS substrate, has strong potential applications in clinical diagnostics, and could be integrated within a real-world pathogen detection workflow.

This presents new capabilities in label-free bacterial detection including novel culture-free investigation capabilities, and an improved methodology for sample handling with minimal preparation and processing.

Keywords: Bacterial identification, Raman spectroscopy, MX-Raman, SERS, nanoparticle monolayer,

1. INTRODUCTION

Enhanced Spectroscopies and Nanoimaging 2022, edited by Prabhat Verma, Yung Doug Suh,
Proc. of SPIE Vol. 12203, 1220303 · © 2022 SPIE ·
0277-786X · doi: 10.1117/12.2635324

Cystic fibrosis (CF) is an autosomal recessive genetic disorder, affecting 1.37 births per 10,000 in the UK [1]. Diagnosis of secondary bacterial infections in CF is skill-intensive, relying on skilful manipulation of complex sputum samples and placing a significant burden on healthcare providers. Among all CF lung infections, 81% are caused by *Pseudomonas aeruginosa*, whilst another 30% are at least partly attributable to *Staphylococcus aureus*, both of which are concerning due to increasing resistance to common antibiotics [2]. For diagnostic methods dependent on cell culture, the period from patient sampling to analysis of results takes between 12 hours and 5 days, which leads to delays in treatment and adverse patient outcomes.

Raman spectroscopy can provide a highly characteristic optical fingerprint of a target but is inherently limited by weak Raman scattering [3]. Surface enhanced Raman scattering (SERS) approaches to bacteria identification can improve signal generation [4], but substrate quality and cost are key limiting factors in further use of the method. SERS for bacterial detection has been demonstrated in both laboratory [5]–[8] and clinical settings [9], demonstrating distinction at both species level [5]–[7] and strain level [8], [10]. Reliance on complex fabrication methods for plasmonic substrates limits scalability and real-world application, while poor control of fabrication conditions leads to low SERS signal uniformity and reproducibility for low-cost nanoparticle assembly methods [4].

We report the development and application of a novel multi-excitation surface enhanced Raman spectroscopy-based methodology (MX-SERS) for label-free and non-invasive detection of microbial pathogens that can be used with unprocessed clinical samples directly to provide rapid pathogen identification and disease diagnosis. MX-SERS relies on the differential excitation of non-resonant and resonant molecular components in bacterial cells to enhance the molecular finger-printing capability to obtain strain level distinction in bacterial species. Resonance Raman contributions to MX-SERS, resulting from excitation at different laser wavelengths, are observed from carotenoids and porphyrins.

Here we demonstrate a simple and low-cost fabrication method to produce highly reproducible and uniform SERS-active substrates that can be adapted to fit a chosen wavelength regime, and hence use MX-SERS to detect and characterise the respiratory pathogens *P. aeruginosa* and *S. aureus* as typical infectious agents associated with cystic fibrosis. By combining highly informative MX-SERS spectra with multivariate analysis (Principle component analysis, PCA) and supervised classification (support vector machine, SVM), classification accuracy was found to be >99% for both species investigated, including 100% accuracy for *S. aureus*.

The results demonstrate that MX-SERS is a highly sensitive optical fingerprinting that can quickly identify bacterial species, indicating further that this can form the basis of a powerful platform for rapid and culture-free detection and diagnosis of clinical pathogens, in this case relevant to cystic fibrosis. Such a platform could provide translatable diagnostic solutions in a variety of disease areas and could further be utilised for the rapid detection of anti-microbial resistance.

1.1 Raman and SERS spectra of Bacteria

There are different origins for Raman and SERS spectra from bacteria [4], [9], [11]. Raman spectra of bacteria are an average measure of a whole sample, since the illumination source is scattered by all of the material present in the focal volume (**Figure 1a**). This provides information from both interior and surface components of a cell or group of cells.

In contrast, SERS signals from bacteria are only produced from cellular material present in the enhanced electric field immediately surrounding the nanostructured surface, on a plasmon-active surface (**Figure 1b**) [4], [9], [11]. SERS spectra can be acquired considerably faster than equivalent Raman spectra (acquisition in ms to s) and with lower laser powers, minimising the potential for sample damage by the laser. The increase in sensitivity, and lack of time-consuming sample preparation, means SERS is particularly suitable for microbial detection and analysis where quick initial or preliminary identification may be required. Identification of bacterial species and strain is the first step in creating an open library of bacterial SERS spectra that would allow quick identification of bacterial contaminants in any sample.

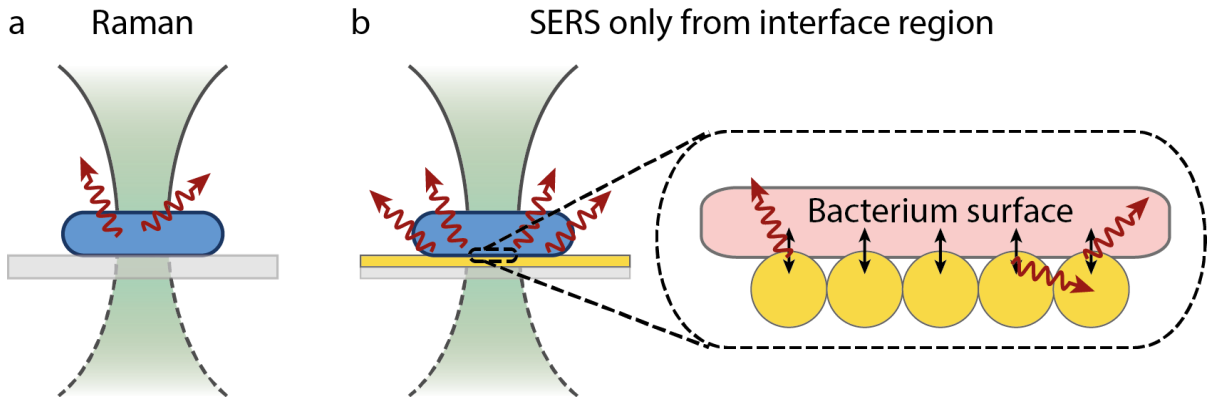

Figure 1 Origin of bacteria Raman and SERS signals. (a) Raman signals produce an average measure of the whole cell. (b) SERS signals produce a stronger signal, but only from the interface of the cell and the nanostructured surface.

1.2 MX-SERS

Multi-excitation surface enhanced Raman spectroscopy (MX-SERS) is a further development from our own work, MX-Raman [12]. Briefly, SERS spectra are acquired from a sample on a nanostructured plasmonic substrate (**Figure 2a**) at a multitude of wavelengths (**Figure 2b**). Both MX-Raman and MX-SERS use the strong wavelength dependence of the Raman scattering cross-section, and the resulting changes to relative Raman peak intensities, to improve sample distinction and classification. MX-SERS further makes use of the wavelength dependence of the surface plasmon, which is used in this work to demonstrate a novel capability in bacterial identification, providing species information beyond that of standard Raman and SERS spectroscopy.

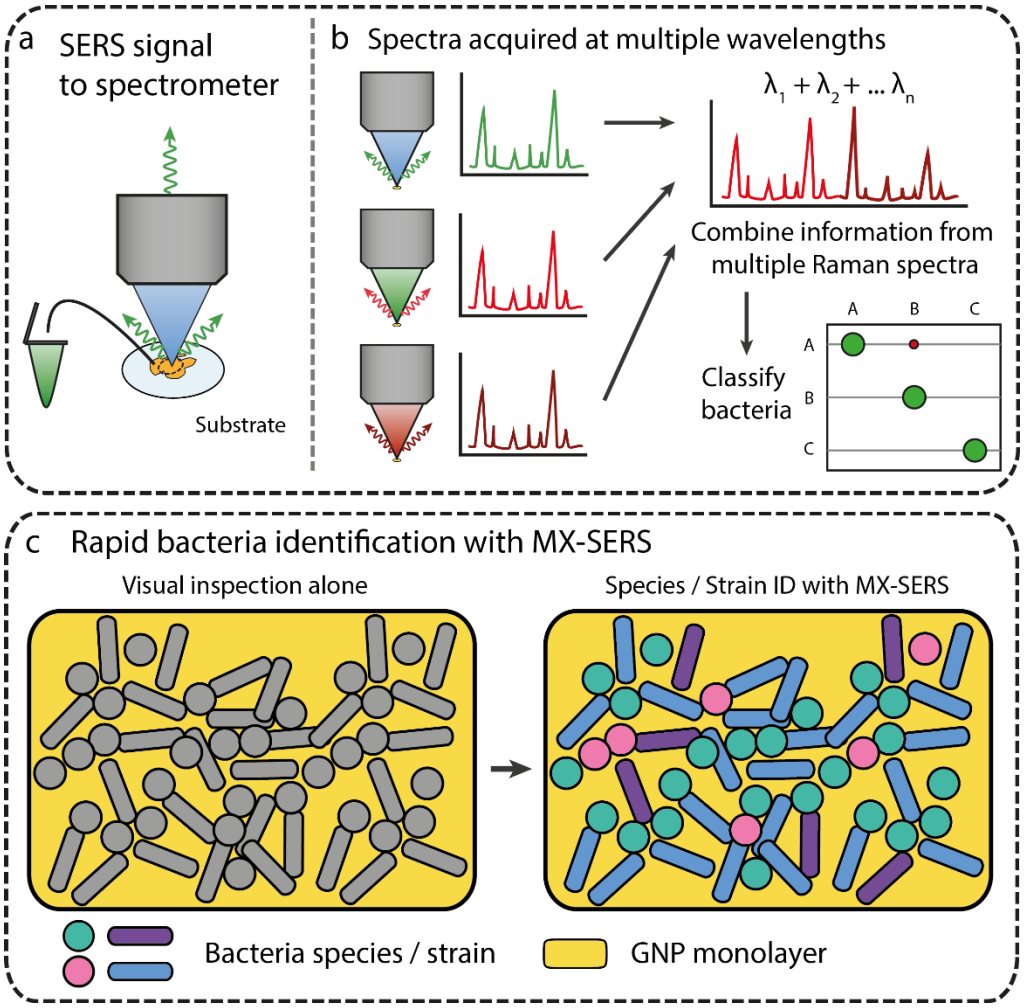

Figure 2 Visual explanation of MX-SERS for bacteria identification. (a) A sample of bacteria is placed on a nanostructured plasmonic substrate, and laser excitation. (b) Spectra are acquired at a multitude of excitation wavelengths, and the spectral information combined to improve classification. (c) Compared to visual inspection alone, which can provide morphological information, MX-SERS can provide bacteria identification with species and strain level specificity.

2. MATERIALS AND METHODS

2.1 Instrumentation

Raman and SERS spectromicroscopy measurements were carried out using a Renishaw InVia microscope system, equipped with a spectrometer, an upright microscope (Leica DM 2500-M), and excitation lasers at 405 nm, 532 nm, 660 nm and 785 nm (Renishaw Plc.). Typical laser powers for SERS data acquisition were between 0.025% (25 μW) and 0.1% (100 μW), with an exposure time of between 0.5 s and 2 s per spectrum and with one accumulation.

The spectrometer was equipped with a Leica DMLM series microscope. Scattered light at the sample was collected using a microscope objective with a 50× magnification, which has a short working distance (0.37 mm, numerical aperture 0.75) and creates a small diameter laser spot (1.2 μm). The spectrometer grating was calibrated by measuring the position of the most prominent band from a silicon (111) wafer (520.6 cm^{-1}).

2.2 SERS substrate preparation

GML fabrication is based on work by Reincke et al. [13]. A schematic description of the substrate preparation process is shown in (**Figure 3a**). Gold nanoparticle solution (2 mL, BBI Solutions, CV ≤ 8%) was added to a 25mm glass petri dish. Cyclohexane (Sigma-Aldrich, Chapter 7 130 2mL) was pipetted onto the gold, forming a biphasic system. Ethanol (Sigma-Aldrich, 750μL) was pipetted directly into the gold layer, taking care to deliver the aliquot swiftly, but without disrupting the two layers and cause mixing. This addition promoted the formation of a monolayer of nanoparticles at the liquid-liquid interface. After formation of a stable monolayer, the organic phase was gently removed by pipetting (**Figure 3b**). This both exposed the monolayer to the air and promoted close packing of gold nanoparticles within the monolayer. A glass coverslip was cleaned in isopropyl alcohol (Sigma-Aldrich), in cyclohexane, and then in ethanol, to remove any surface contaminants, and then dried under gentle air flow. The coverslip was then carefully inserted into the aqueous layer using tweezers, and slowly removed, allowing the monolayer of gold nanoparticles to adhere to the surface. After successful transfer of the monolayer, the coverslip was allowed to dry under ambient conditions, inside a container to prevent dirt and dust from coming into contact with the newly prepared surface. This fabrication process produced a close-packed nanostructured monolayer of gold nanoparticles on the glass surface, henceforth, called the gold monolayer (GML) substrate (**Figure 3c**).

For substrate characterisation, GML substrates were functionalised with 4-mercaptobenzoic acid (MBA). Briefly, GML substrates were immersed in an ethanolic solution of MBA (10 μM, 1074-36-8, Sigma Aldrich) for 12 hours to ensure complete surface coverage. Before use, GML substrates were removed from solution, and rinsed with ethanol to remove unbound MBA, before drying under ambient conditions.

2.3 Bacterial sample preparation

Bacterial samples were grown overnight in LB broth (Formedium, UK), for 18 hours at 37°C and with shaking at 130rpm. *S. aureus* was grown with aeration, *P. aeruginosa* was grown without aeration. Bacterial culture absorbance was measured using a Hitachi U-2001 spectrophotometer at 600nm, and samples were diluted with LB broth to reach OD_{600} = 0.4. Bacterial samples were washed three times with centrifugation and resuspended in deionised (DI) water to remove residual culture media that might contribute to the Raman spectra. Samples were then diluted by a factor of ten. 20μL of the diluted suspension was pipetted directly onto the GML substrate and dried at room temperature. This process yielded large regions of the GML substrate that were covered with a single layer of bacterial cells on the gold monolayer.

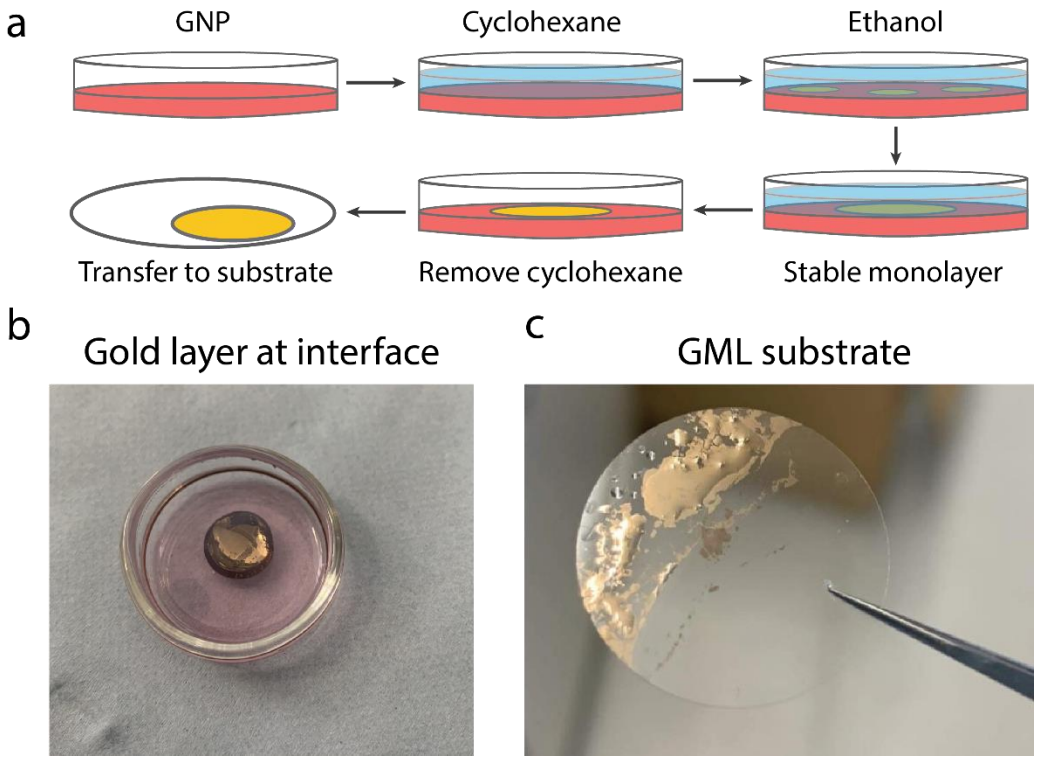

Figure 3 GML substrate fabrication method. (a) Illustration of fabrication process (see methods for detail). (b) Image of gold nanoparticle monolayer at the liquid-liquid interface. (c) Large-area GML on glass coverslip (d = 20mm).

2.4 Data processing and analysis

Cosmic rays were removed using Wire software (Version 3.1) from Renishaw. Spectra were wavelet denoised, and fitted with a 9th order polynomial baseline subtraction using the iRootLab toolbox for Matlab [14], then normalised. Raman spectra contain a large amount of data, and large multidimensional spectra datasets cannot be readily visualized. Dimensionality reduction of the dataset was used to improve visualisation and preserve key features and subtle differences within the underlying data.

Multivariate statistical analysis (PCA) and SVM were carried out on the pre-processed data using iRootLab. For PCA, data was normalised to maximum intensity and mean centred prior to analysis, and the first ten PCs were generated for each spectrum. For SVM analyses, a k-fold cross-validation method was used (K = 10) to train the classifier on smoothed and maxima-normalised spectral data. Training used the default parameters of the software (Number of refinements: 1, max moves per refinement: 3, c: $10^{-1} – 10^{7}$, γ: $10^{-7} – 10$).

Data was plotted in GraphPad Prism 8.0.1, and figures were prepared in Adobe Illustrator.

3. CHARACTERISATION OF SERS-ACTIVE SUBSTRATES

Fabrication of high-quality and effective SERS-active substrates from an assembly of nanoparticles is often challenging, as reproducible and uniform SERS signal generation depends on the uniform formation of SERS-active hotspots across the surface [15]. We decided to explore whether a highly uniform SERS substrate could be produced with low complexity and low cost, to facilitate future use in a real-world bacteria analysis workflow. The GML substrates were characterised, focussing on the SERS signal properties of the substrates, and evaluated for use in bacteria detection.

3.1 SERS substrate uniformity and wavelength dependence

The uniformity of SERS signal generation from GML substrates was evaluated to establish their suitability for reproducible bacteria analysis. Imaging with SEM provided a visual confirmation that a monolayer of gold nanoparticles had formed at the liquid-liquid interface and had been successfully transferred to the glass substrate (**Figure 4a**). However, since small variations in surface features, including in-particle spacing, arrangement and size, has a significant impact on the plasmonic properties of the nanostructured surface, SERS spectra were used for a more conclusive evaluation of substrate quality [15].

SERS spectral maps were acquired from GML substrates functionalised with 4-mercaptobenzoic acid (MBA), and good uniformity and reproducibility was demonstrated across the full dataset (**Figure 4b**). The mean and standard deviation of the ν12a and ν8a ring breathing modes, at 1077 cm^{-1} and 1588 cm^{-1} respectively (see **Table 1**), were used to assess the uniformity and reproducibility of the SERS signal intensity (**Figure 4c,d**) [16]. The average RSD value across 27 spectral maps (each of 400 spectra) was 15.6% at 1077 cm^{-1}, and 15.7% at 1588 cm^{-1}, indicating good SERS signal uniformity across the surface (**Figure 4e**). Reproducibility between substrates is indicated by the mean intensity (**Figure 4f**).

Table 1 SERS peak assignment of 4-Mercaptobenzoic Acid [16]

Raman shift / cm^{-1}	Assignment
718	γ(CCC)
840	δ(COO^-)
1080	ν_{12} (Aromatic ring)
1370-1380	ν_s(COO^-)
1590	ν_{8a} (Aromatic ring)
1710	ν(C=O)

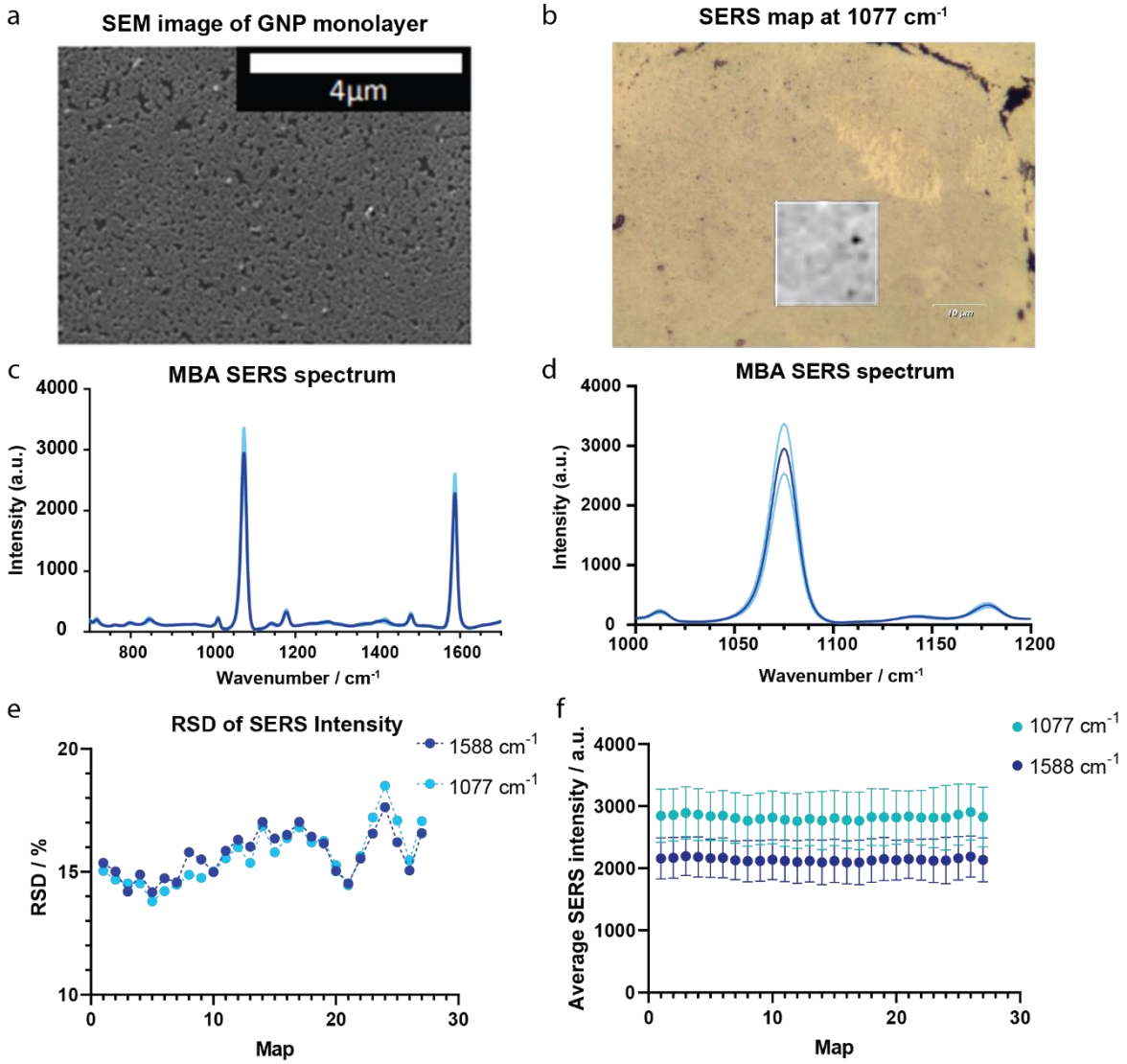

Figure 4 Characterisation of SERS monolayer. (a) SEM image of the gold monolayer on glass substrate. (b) SERS intensity map of MBA signal at 1077 cm^{-1} (grey) overlaid on brightfield image of GML substrate. (c) Average (n=400) SERS spectrum of MBA-modified gold monolayer substrate, with zoomed spectral region shown in (d). (e) RSD of SERS signal from image maps of substrates (average 15.6% at 1077 cm^{-1} and 15.7% at 1588 cm^{-1}). (f) Average intensity of SERS signal from 27 SERS maps at 1077 cm^{-1} and 1588 cm^{-1}.

3.2 Wavelength dependence

MX-Raman exploits the differing wavelength-dependence properties of the Raman scattering cross section, and hence, is intrinsic to a material [12]. The overall wavelength dependence of MX-SERS must also account for the plasmonic properties of the surface, and the extent to which individual vibrational modes are enhanced at the nanostructured surface. The choice of excitation wavelength and detection wavelength band can be clearly observed in **Figure 5**. SERS spectra were acquired at 405 nm, 532 nm, 660 nm, and 785 nm from an MBA- functionalised GML substrate. As expected, the strongest SERS signals were obtained from excitation at 785 nm, and effectively no signal was

obtained using 405 nm excitation, matching the known useful wavelength range for nanostructured surfaces made from gold [17]. SERS signal intensity was more than 10x stronger using excitation 660 nm and 785 nm excitation compared to 532 nm excitation, so excitation at 660 nm and 785 nm was used to acquire SERS spectra of bacterial samples in the remainder of this work.

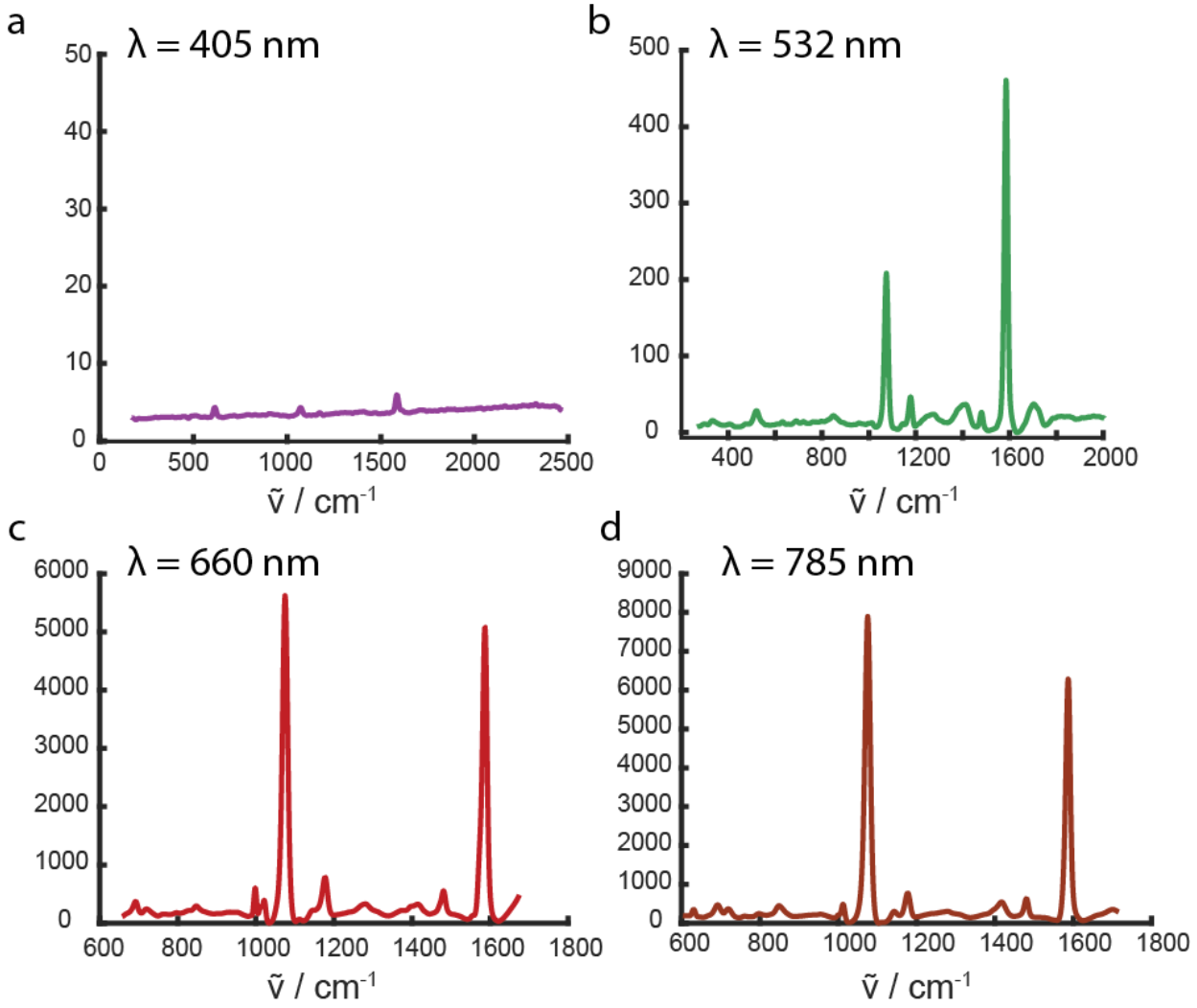

Figure 5 Wavelength dependence of SERS MBA signal. Average SERS spectra (n=400) acquired from an MBA-functionalised GML substrate using laser excitation at (a) 405 nm, (b) 532 nm, (c) 660 nm and (d) 785 nm.

Having characterised the GML substrates and evaluating their performance with MX-SERS, we wanted to investigate whether this improved bacterial classification.

4. MX-SERS FOR ENHANCED BACTERIA SENSING

We next explored the use of GML SERS substrates for bacterial identification with MX-SERS. Based on measurements of GML substrates functionalised with MBA, we decided to use 660 nm and 785 nm excitation to explore MX-SERS, rather than the 532 nm and 785 nm combination of laser excitation that had previously been used to explore MX-Raman. Distinct features were observed from spectra acquired with each excitation wavelength (**Figure 6a,b**), indicating the wavelength dependence of SERS and the increased information content provided by use of a multitude of spectra should improve classification accuracy compared to SERS acquired with a single excitation wavelength, similar to our prior experiences with MX-Raman [12]. Spectral analysis for MX-SERS was based on the combined 660 nm and 785 nm datasets (**Figure 6c**). SERS spectral maps acquired using 660 nm and 785 nm excitation were taken from the same sample region, ensuring that any local variations in SERS signal across the spectral map and between the two excitations were accounted for in the dataset. PCA was performed on all datasets, showing that differences in spectral signatures result in distinct clusters for spectra of the two bacteria (**Figure 6d,e,f**). A support vector machine was trained for spectral classification with 10-fold cross-validation (see methods for details), showing a clear improvement in classification accuracy using MX-Raman (**Figure 6g,h,i**).

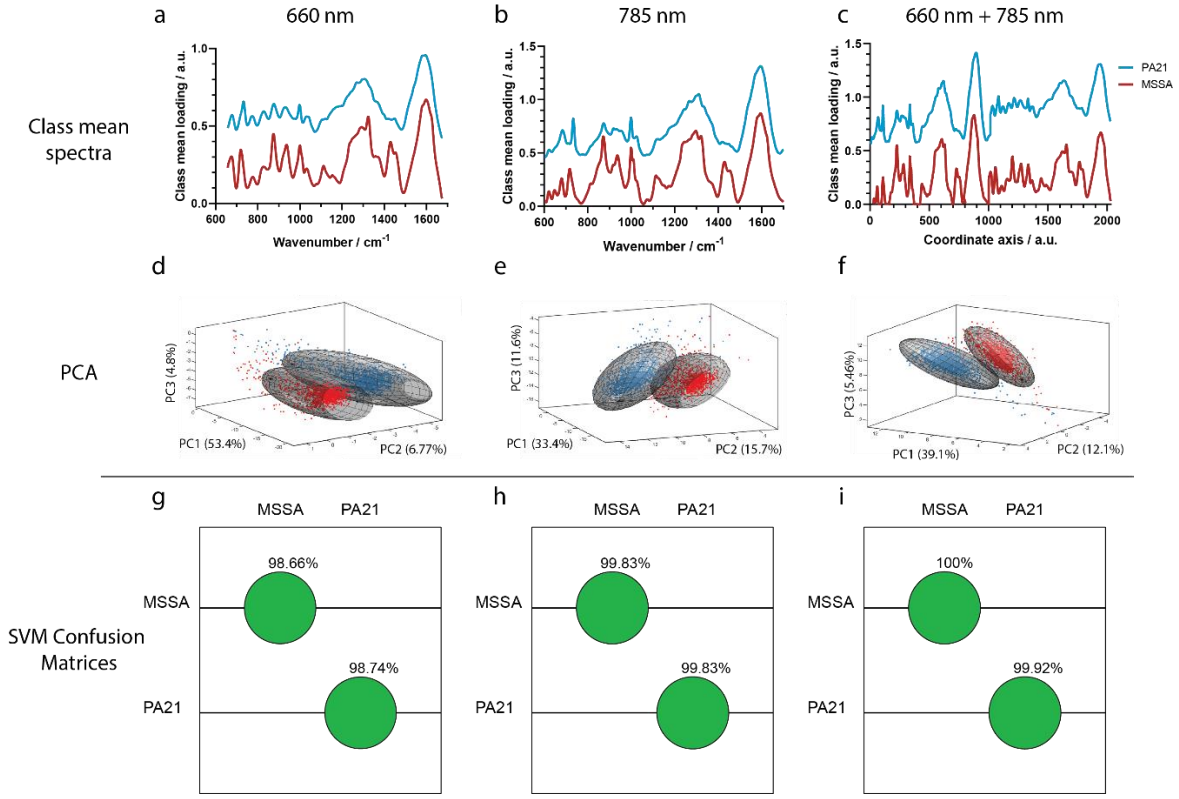

Figure 6 Improved bacteria classification accuracy using MX-SERS. SERS spectra of MSSA (n=1200) and PA21 (n=1200) were acquired using **(a)** 660 nm and **(b)** 785 nm excitation, and were combined **(c)** for MX-SERS analysis. **(d,e,f)** Distinct clusters were observed from 3D plots of the first 3 principle components resulting from PCA in all cases. **(g,h,i)** The highest SVM classification accuracy was achieved for both PA21 and MSSA using MX-SERS.

5. CONCLUSIONS & FUTURE OUTLOOK

Results of bacterial analysis with MX-SERS demonstrated a clear improvement in classification accuracy compared to analysis of SERS spectra acquired at a single wavelength (660 nm and 785 nm). Analysis of the GML substrates demonstrates that they can be used to generate high quality SERS spectra, with good reproducibility between substrates and uniform SERS signal from within a substrate. Classification accuracy using MX-SERS spectra was found to be >99% for both species investigated, including 100% accuracy for S. aureus. A high-quality SERS substrate that combines easy fabrication with uniform and reproducible SERS signal generation is essential for future application in real-world settings. Work is ongoing to develop capabilities in handling sputum samples directly on GML SERS substrates, aiming to directly detect and identify bacteria whilst avoiding confounding signals from other components of the complex sputum matrix. Current diagnostic methods rely on cell culture, a key bottleneck in microbiological analysis, inherently limiting the speed of many standard laboratory diagnostics. MX-SERS requires only small numbers of bacteria for analysis, and although sample processing is required to isolate target bacteria, this processing remains faster than cell culture-based approaches. Avoiding this bottleneck by use of a method that does not depend on cell culture has the potential to provide a route to rapid and adaptable diagnostics in real-world healthcare settings.

REFERENCES

[1] P. M.Farrell, "The prevalence of cystic fibrosis in the European Union," *J. Cyst. Fibros.*, vol. 7, no. 5, pp. 450–453, 2008, doi: 10.1016/j.jcf.2008.03.007.

[2] N. Høiby and B. Frederiksen, "Microbiology of cystic fibrosis," in *Cystic Fibrosis*, 2nd ed., M. E. Hodson and D. M. Geddes, Eds. London, United Kingdom: Arnold, 2000, pp. 83–107.

[3] L. Wang *et al.*, "Applications of Raman Spectroscopy in Bacterial Infections: Principles, Advantages, and Shortcomings," *Front. Microbiol.*, vol. 12, 2021, doi: 10.3389/fmicb.2021.683580.

[4] C. L. Haynes, A. D. McFarland, and R. P. Van Duyne, "Surface-Enhanced Raman Spectroscopy," *Anal. Chem.*, vol. 77, no. 17, p. 338, 2005, doi: 10.1021/ac053456d.

[5] R. M. Jarvis and R. Goodacre, "Discrimination of bacteria using surface-enhanced Raman spectroscopy," *Anal. Chem.*, vol. 76, no. 1, pp. 40–47, 2004, doi: 10.1021/ac034689c.

[6] R. M. Jarvis, A. Brooker, and R. Goodacre, "Surface-enhanced Raman scattering for the rapid discrimination of bacteria.," *Faraday Discuss.*, vol. 132, no. 0, pp. 281–292; discussion 309-319, 2006, doi: 10.1039/b506413a.

[7] G. Naja, P. Bouvrette, S. Hrapovic, and J. H. T. Luong, "Raman-based detection of bacteria using silver nanoparticles conjugated with antibodies," *Analyst*, vol. 132, pp. 679–686, 2007, doi: 10.1039/B701160A.

[8] A. Walter, A. März, W. Schumacher, P. Rösch, and J. Popp, "Towards a fast, high specific and reliable discrimination of bacteria on strain level by means of SERS in a microfluidic device," *Lab Chip*, vol. 11, pp. 1013–1021, 2011, doi: 10.1039/C0LC00536C.

[9] W. R. Premasiri, D. T. Moir, M. S. Klempner, N. Krieger, G. Jones, and L. D. Ziegler, "Characterization of the Surface Enhanced Raman Scattering (SERS) of Bacteria," *J. Phys. Chem. B*, vol. 109, no. 1, pp. 312–320, 2004, doi: 10.1021/jp040442n.

[10] K. E. Stephen, D. Homrighausen, G. DePalma, C. H. Nakatsu, and J. Irudayaraj, "Surface

enhanced Raman spectroscopy (SERS) for the discrimination of Arthrobacter strains based on variations in cell surface composition," *Analyst*, vol. 137, pp. 4280–4286, 2012, doi: 10.1039/C2AN35578G.

[11] S. Efrima and L. Zeiri, "Understanding SERS of bacteria," *J. Raman Spectrosc.*, vol. 40, no. 3, pp. 277–288, 2008, doi: 10.1002/jrs.2121.

[12] A. P. Lister *et al.*, "Multi-Excitation Raman Spectroscopy for Label-Free, Strain-Level Characterization of Bacterial Pathogens in Artificial Sputum Media," *Anal. Chem.*, vol. 94, no. 2, pp. 669–677, Jan. 2022, doi: 10.1021/acs.analchem.1c02501.

[13] F. Reincke, S. G. Hickey, W. K. Kegel, and D. Vanmaekelbergh, "Spontaneous Assembly of a Monolayer of Charged Gold Nanocrystals at the Water/Oil Interface," *Angew. Chemie*, vol. 43, no. 4, pp. 458–462, 2004, doi: 10.1002/anie.200352339.

[14] J. Trevisan, P. P. Angelov, A. D. Scott, P. L. Carmichael, and F. L. Martin, "IRootLab: a free and open-source MATLAB toolbox for vibrational biospectroscopy data analysis," *Bioinformatics*, vol. 29, no. 8, pp. 1095–1097, 2013, doi: 10.1093/bioinformatics/btt084.

[15] Y. Wang and E. Wang, "Nanoparticle SERS Substrates," in *Surface Enhanced Raman Spectroscopy: Analytical, Biophysical and Life Science Applications*, S. Schlücker, Ed. Wiley-VCH Verlag GmbH & Co. KGaA, 2010, pp. 39–69.

[16] A. Michota and J. Bukowska, "Surface-enhanced Raman scattering (SERS) of 4-mercaptobenzoic acid on silver and gold substrates," *J. Raman Spectrosc.*, vol. 34, no. 1, pp. 21–25, Jan. 2003, doi: 10.1002/jrs.928.

[17] S. Schlücker, "SERS Microscopy: Nanoparticle Probes and Biomedical Applications," in *Surface Enhanced Raman Spectroscopy: Analytical, Biophysical and Life Science Applications*, 1st ed., S. Schlücker, Ed. Wiley-VCH Verlag GmbH & Co. KGaA, 2010, pp. 263–283.